1,7-, 1,6-, and 1,6,7- Derivatives of Dodecylthio Perylene Diimides: Synthesis, Characterization, and Comparison of Electrochemical and Optical Properties

Adrian J. Riives[1], Zhaorui Huang[1], Nathaniel T. Anderson[1], and Peter H. Dinolfo[1] *

[1] Department of Chemistry and Chemical Biology, Rensselaer Polytechnic Institute, 110 Eighth Street, Troy, New York 12180, United States

Email: dinolp@rpi.edu

Abstract

The synthesis, separation, and characterization of 1,6-, 1,7-, and 1,6,7- derivatives of dodecylthio–N,N'–(2,4–diisopropylphenyl)-3,4,9,10-perylenetetracarboxylic diimide are reported. The three derivatives display noticeable differences in their electronic absorption and emission properties, with a bathochromic shift in spectral maxima from **1,6–Thio–PDI**, to **1,7–Thio–PDI**, to **1,6,7–Thio–PDI**. The **1,7–Thio–PDI** derivative had the highest fluorescence quantum yield and longest fluorescence lifetime in toluene (Φ_F = 0.85, τ_F = 8.3 ns), followed by **1,6–Thio–PDI** (Φ_F = 0.54, τ_F = 6.6 ns) and **1,6,7–Thio–PDI** (Φ_F = 0.16, τ_F = 4.4 ns). The difference in dipole moment between the ground and excited states were estimated by the Lippert-Mataga analysis of solvent dependent absorption and emission properties and ranged from $\Delta\mu$ = 7.1 Debye for **1,6,7–Thio–PDI** to 8.3 Debye for **1,6–Thio–PDI**. These measurements were supported by time–dependent density functional theory calculations, which helped interpret the differences in absorption spectra. Cyclic voltammetry showed minor differences in the reduction potentials for the singly and doubly reduced states. The absorption spectra of the singly and doubly reduced states are also reported.

Introduction

Perylene-3,4,9,10-tetracarboxylic diimide and their derivatives, also referred to as perylene diimides (PDIs), are robust organic chromophores which have garnered significant attention in both commercial and academic research.[1,2] PDIs have been utilized since the 1950s as high performance dyes and pigments due to their exceptional chemical, photo, and thermal stability,[2] as well as their high tinctorial strength that allows for hues ranging from red to purple.[3] PDIs possess excellent photochemical properties, such as good electron mobility, tunable absorption spectra, excellent stability to photooxidation,[4] and high fluorescence quantum yields.[1] This range of chemical properties make PDIs attractive for a variety of applications. For example, PDIs have been applied towards fingerprint detection,[5] heparin detection,[6] photodynamic therapy,[7] and live cell staining.[8] Additionally, due to their excellent optical properties and relatively high electron affinity,[9,10] PDIs have been studied for use in photovoltaic applications,[11–13] light emitting diodes,[14,15] light-harvesting arrays,[16–18] fluorescent solar collectors,[19,20] organic field-effect transistors,[21,22] and dye sensitized solar cells.[23–25] Notably, one group citing a 17% efficiency in a single junction organic solar cell incorporating PDIs.[26]

The excellent chemical properties of PDIs and their vast potential utility is largely due to their readily derivatizable structure. The PDI moiety contains a rigid π conjugated core comprised of two naphthalene half units, providing three distinct regions for chemical modification, the bay (1,6,7,12), ortho (2,5,8,11) and imide positions.[1,2,9] Chemical modifications at the bay positions tunes the electrical and optical properties within the PDI due to the significant HOMO and LUMO coefficients at these positions. The addition of π donating functional groups stabilizes the HOMO, whereas π accepting groups stabilize the LUMO.[1] Conversely, chemical modifications to the imide region do not alter the electrical or optical properties of the PDI significantly because nodes in the HOMO and LUMO orbitals are centered at the imide nitrogen.[27] Instead, chemical modifications at the imide region are used to increase the solubility of PDIs in organic solvents. This increased solubility is important because PDIs and their precursors are notoriously insoluble in most organic solvents due to their tendency to aggregate via face-to-face π-π stacking. [1,2,9,28]

While PDIs have been utilized industrially since the 1950s, chemical utility for more specific purposes have been limited by their planar structure, which lends itself to π- π stacking, and thus causes solubility issues. In 1997, BASF disclosed a patent[29] for the bromination of perylene-3,4,9,10-tetracarboxylic dianhydride (PTCDA) to yield 1,7-dibromoperylene-3,4,9,10-tetracarboxylic dianhydride (1,7-Br–PTCDA). The 1,7-dibromo PDI provides an excellent starting compound for further nucleophilic or metal catalyzed cross-coupling reactions which can be utilized to achieve desired functionality and improve the PDI's solubility in organic solvents. Following this disclosure, researchers utilized the bromination procedure to functionalize the bay positions with numerous functional groups, including phenoxy, pyrrolidinyl, alkyl, aryl, and aryloxy groups, among others.[1,2,9] In 2004 it was discovered[30] that the BASF bromination procedure of PTCDA was not regioselective for 1,7-dibromo–PTCDA, but also lead to the formation of 1,6-dibromo–PTCDA as well as the 1,6,7- and 1,6,7,12-brominated derivatives in minor amounts depending on the specific conditions employed.[30] Since 2004, a select number of publications described the isolation and comparison between the photo– and electrochemical properties of 1,6– and 1,7–PDI regioisomers with different substituents. These substituents include phenoxy,[31] pyrrolidinyl,[30–32] piperidinyl,[33] aryl,[34] fluorenyl,[35] alkynyl,[36] alkyl,[36] and thioether.[37]

We have previously reported the synthesis of N,N'-dipropargyl–perylenediimides with phenoxy, dodecythio, and pyrolidine bay functionalization.[18] These materials were used for the assembly of panchromatic multilayer thin films on oxide surfaces and were designed to examine energy transfer between donor–acceptor layers with the goal of developing solar light harvesting arrays, as well as tunable electrochromic materials. During the synthesis of the N,N'-dipropargyl-di(dodecylthio)perylene–3,4:9,10-bis(dicarboximide), we observed the formation of regioisomers corresponding to the 1,6– and 1,7– isomers. These regioisomers showed noticeably different electronic absorption and emission spectra. In an effort to better understand the differences in excited state properties of these regioisomers and how they may impact the performance of a light harvesting array, we chose to explore these compounds in greater detail.

Herein we describe the synthesis and isolation of the 1,6– and 1,7– regioisomers bis-dodecylthio-PDIs (**1,6-Thio-PDI** and **1,7-Thio-PDI**) and one tris-dodecylthio-PDI (**1,6,7-Thio-PDI**) with bulky diisopropyl substituents at the imide position. While 1,7– and 1,6–difunctionalized PDIs are well reported in the literature, 1,6,7– substituted derivatives are relatively rare which is likely due to the low yield of 1,6,7– Br–PTCDA in the bromination reaction. We also compare the solvatochromic effect on the electronic absorption and emission properties between these derivatives, as well as their electrochemical reduction potentials and absorption spectra of the singly and doubly reduced states.

Results and Discussion

Synthesis and Characterization

The synthetic scheme to form **1,6-Thio-PDI**, **1,7-Thio-PDI**, and **1,6,7-Thio-PDI** is shown in Figure 1 and follows our previously reported method.[18] A mixture of **Br–PTCDA** derivatives was obtained from **PTCDA** following the basic bromination procedure outlined in the BASF patent.[29] Imidization with 2,6–diisopropylaniline gave the corresponding mixture of **Br–PDI** derivatives. During purification at this step, thin layer chromatography showed spots that corresponded to the individual derivatives, however these were not isolated at this point. The mixture was then reacted with dodecanethiol and sodium hydroxide in refluxing pyridine to give the final products. The **1,6-Thio-PDI**, **1,7-Thio-PDI**, and **1,6,7-Thio-PDI** derivatives were separated using a combination of column chromatography and preparatory thin layer chromatography. ^{1}H NMR analysis of the crude reaction product provided relative yields of 90% for **1,7-Thio-PDI**, 9% for **1,6-Thio-PDI**, and less than 1% yield for **1,6,7-Thio-PDI**. These values are consistent with previous reports in literature regarding the formation of 1,6- and 1,7-Thio-PDI regioisomers from **Br–PTCDA**.[30]

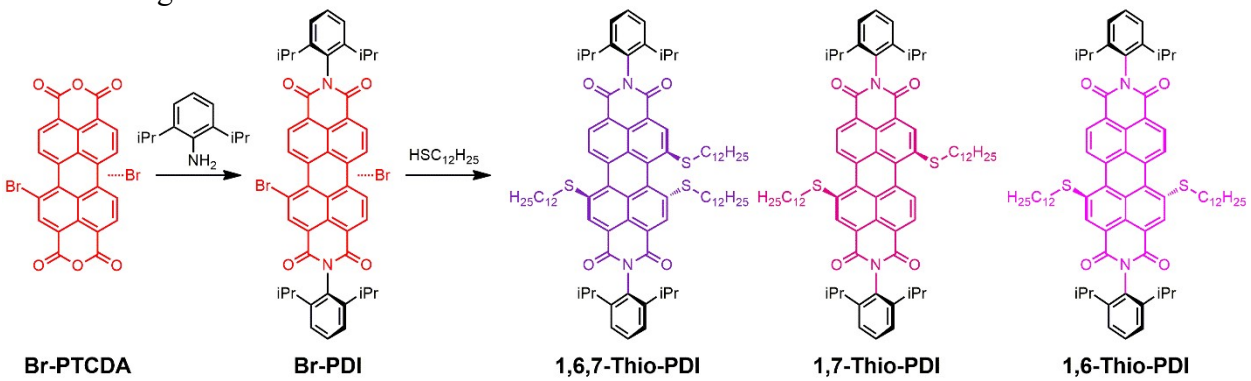

Figure 1. Synthesis of **1,6,7-Thio-PDI**, **1,7-Thio-PDI**, and **1,6-Thio-PDI**, starting from **Br–PTCDA**, followed by imidization with diisopropylaniline, and finally substitution with dodecanethiol.

The purity of the three Thio-PDI derivatives were confirmed by ^{1}H NMR spectra as shown in Figure 2. ^{1}H NMR is particularly useful in the analysis of different PDI derivatives [31] by comparing the signals within the 8.7 – 9.0 ppm range that corresponds to the perylene bay protons, and 7.2-7.6 ppm range for the 2,4–diisopropylphenyl additions at the imide positions. **1,7-Thio-PDI** is identifiable from the others through a doublet-singlet-doublet (d–s–d) splitting pattern observed from 8.75 to 8.95 ppm. The two doublets correspond to the 5–H and 6–H positions and the singlet is assigned to 2–H next to the thio substitutions. The spectrum also shows well resolved peaks for the diisopropylphenyl consistent with the C_2 symmetric structure. This d–s–d pattern for the perylene bay protons has been previously reported for a variety of 1,7-PDI isomers.[30,36,38] However, this is not the case for all varieties of PDI bay substituents as the addition of bulkier groups can shift the peaks, leading to a distortion in the expected d-s-d splitting pattern.[31,39–41]

The **1,6-Thio-PDI** shows a d–d–s pattern for the bay protons and a splitting of diisopropylphenyl peaks due to the asymmetry of the molecule. The signals for the 7(12)–H and 8(11)–H protons at 8.9 ppm display the roofing effect as the coupling constant between two peaks (8 Hz) approaches the magnitude of the difference in chemical shifts (15 Hz). **1,6,7-Thio-PDI** shows two doublet peaks for the 11–H and 12–H and singlets for the remaining bay protons, consistent with the expected structure. The diisopropylphenyl peaks also slightly broader, as comparted with the **1,7-Thio-PDI**, due to the asymmetry of the isomer. Compared to common 1,7-substituted PDIs, splitting patterns of 1,6-PDI and 1,6,7-PDI are not as often reported in literature, as these derivatives are not as readily isolated due to their aforementioned likelihood to occur in much lower yields relative to the 1,7-PDI isomer.[30]

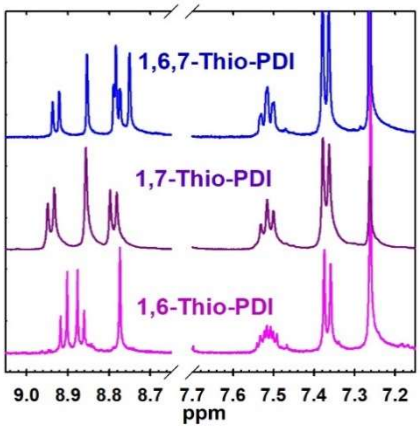

Figure 2. ^{1}H NMR of **1,6-Thio-PDI**, **1,7-Thio-PDI**, and **1,6,7-Thio-PDI** in $CDCl_3$ highlighting the bay proton splitting pattern is located from around 8.7-9.0 ppm, and the diisopropylphenyl proton splitting pattern is located from around 7.3-7.6 ppm. (Spectra were referenced to the residual solvent peak $CHCl_3$ at 7.26 ppm.)

Electronic Absorption

The schematics in Figure 1 shows relative variation in perceived color of the three PDIs derivatives. These dramatic color ranges underscores how the number and symmetry of thio-substituents on the bay positions can lead to variations in perceived color ranging from a dark

magenta for **1,6,7-Thio-PDI**, to a violet purple for **1,7-Thio-PDI**, to purple for **1,6-Thio-PDI**. The normalized absorption and emission spectra of **1,6-Thio–PDI**, **1,7-Thio–PDI**, and **1,6,7-Thio-PDI,** recorded in range of solvents with varying polarity, is depicted in Figure 3. Both the dodecylthio bay and diisopropylphenyl imide substituents aid in excellent solubility in the solvents used here and no evidence of aggregation was observed in the solvents employed here.

The absorption spectra for each Thio-PDI derivative is dominated by intense, broad absorptions in the 500–600 nm range that are characteristic π-π^* transitions. Similar absorption profiles have been observed for other bis–thio substituted PDIs.[37] In toluene, the peak absorption for the S_0-S_1 transition for **1,6-Thio-PDI** occurs at 562 nm, 574 nm for **1,7-Thio-PDI**, and 584 nm for **1,6,7-Thio-PDI**. The absorption profile for **1,7-Thio-PDI** is the narrowest amongst the three derivatives and had a second prominent band at 425 nm. This second band is absent in **1,6-Thio-PDI** and **1,6,7-Thio-PDI**, or likely redshifted relative to **1,7-Thio-PDI** and overlapping S_0-S_1 transition as predicted by TD–DFT calculations (vide infra). The approximate 35 to 60 nm bathochromic shift of these PDIs as compared to unsubstituted versions suggests the thio groups are slightly more π-donating than phenoxy groups, but less than pyrrolidino.[1] Additionally, the broad nature of the absorption bands and lack of clear vibronic structure is consistent with a higher degree of twisting of the perylene core due to the larger sulfur groups.[37] DFT modeling of the derivatives showed a noticeably larger twist angle of the perylene core for **1,6,7-Thio-PDI**, versus the other two (Table 1).

Previous reports comparing the absorption spectra of 1,6- and 1,7-PDI regioisomers have shown that depending on the electron donating or accepting ability of bay functionalization groups, absorption features vary between isomers. Dubey and co–workers isolated the 1,6- and 1,7- regioisomers of both phenoxy and pyrrolidino disubstituted PDIs.[31] In both cases, the 1,7–isomers showed a narrower S_0-S_1 transition in the visible range and a second prominent band towards the UV. Similar to **1,6–Thio–PDI**, their 1,6– isomers lacked the distinct higher energy transition but showed broader visible bands. Similar trends were also observed for 1,6- and 1,7-fluorenyl disubstituted PDIs in a variety of solvents.[35]

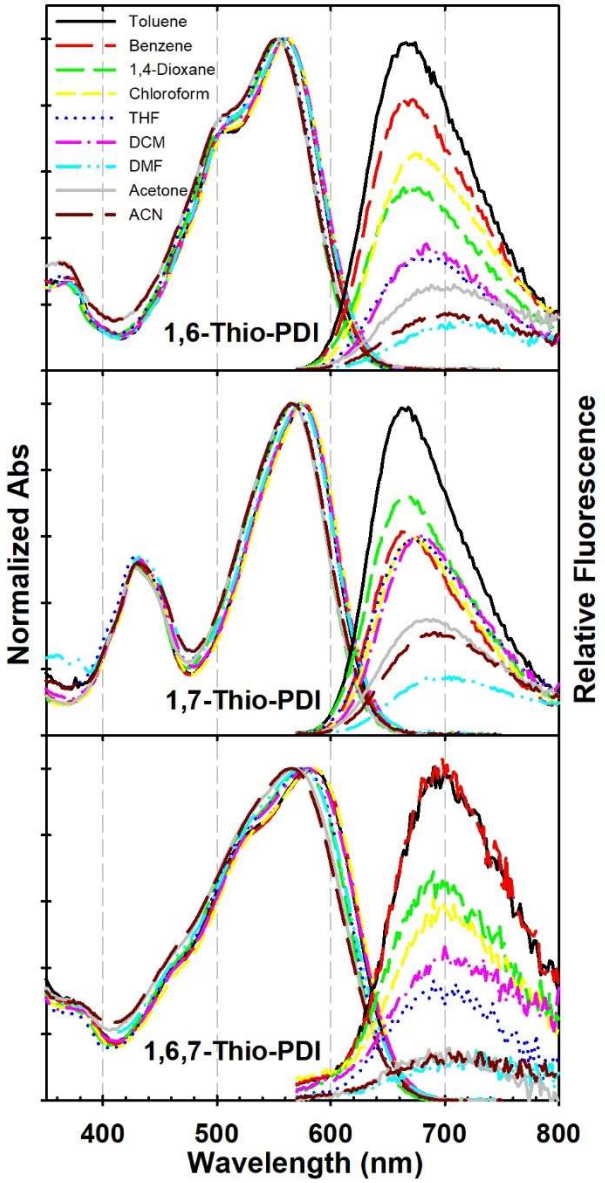

Figure 3. Normalized absorption and emission spectra for **1,6-Thio-PDI** (top), **1,7-Thio-PDI** (middle), and **1,6,7-Thio-PDI** (bottom) in a range of solvents. Each emission spectra (ex 525nm) is scaled relative to the intensity of the sample taken in toluene.

Table 1. Absorption and Emission Parameters for Thio-PDI Derivatives.							
Isomer	λ_{Abs} (nm, Tol)	λ_{Em} (nm, Tol)	Stokes (cm^{-1}, Tol)	Φ_F (Tol)	τ_F (Tol, ns)	τ_F (DMF, ns)	Twist angle (°)
1,6-Thio–PDI	562	668	2820	0.54 ± 0.01	6.3 ± 0.34	2.1 ± 0.12	22.5
1,7-Thio–PDI	574	664	2360	0.85 ± 0.02	8.1 ± 0.09	4.1 ± 0.34	22.1
1,6,7-Thio–PDI	582	696	2780	0.16 ± 0.01	4.4 ± 0.01	2.0 ± 0.11	23.2, 33.5

Table 1. Spectral Parameters of **1,6-Thio-PDI**, **1,7-Thio-PDI**, and **1,6,7-Thio-PDI** in Toluene observed for all parameters such as lifetime (τ), quantum yield (Φ_F), absorbance and emission peaks, and the calculated Stokes shift in wavenumbers (cm^{-1}). The twist angle was calculated

from DFT geometry optimized structures as the dihedral angle between the 6 and 7 (1 and 12) positions on the perylene core.

Emission Properties

The normalized fluorescence emission spectra of **1,6-Thio-PDI**, **1,7-Thio-PDI**, and **1,6,7-Thio-PDI** were recorded in solvents of varying polarity and are included in Figure 3 and the relevant parameters are summarized in Table 1. Each emission spectra is scaled relative to the intensity of the sample taken in toluene, which showed the highest intensity among all the solvents. The emission spectra for each derivative shows a broad, relatively featureless band, with peak maxima at 668 nm for **1,6-Thio-PDI**, 664 nm for **1,7-Thio-PDI**, and 696 nm for **1,6,7-Thio-PDI** in toluene. The Stokes shift also increases from 2,360 cm^{-1} for **1,7-Thio-PDI** to 2,780 cm^{-1} for **1,6,7-Thio-PDI**.

The fluorescence quantum yield, determined in toluene, was highest for **1,7-Thio-PDI** (Φ_F = 0.85), and decreased to 0.54 for **1,6-Thio-PDI** and 0.16 for **1,6,7-Thio-PDI**. These values are intermediate between those typically observed for phenyoxy and amine substituted PDIs.[31] There are only a few reports comparing the quantum yield between 1,6– and 1,7–PDI regioisomers. Dubey et. al found a very small decrease in the quantum yield from a 1,7– to 1,6–regiosomers of a phenoxy PDI (0.97 to 0.96 in toluene), but a much larger difference for pyrollidine sustiuents (0.4 for 17, 0.7 for 16).[31] Dey et. al. found that the quantum yield for 1,7–diaryl–PDIs were generally larger than the 1,6– regioisomers.[34]

As the solvent polarity increases, the emission bands for all three derivatives experience a bathochromic shift and a corresponding decrease in intensity. The fluorescence lifetimes of the three derivatives follows a similar trend, decreasing with an increase in the solvent polarity (toluene vs DMF). The lifetimes also mirror the trends in quantum yield when comparing between differences derivatives. The most symmetrical derivative, **1,7-Thio-PDI**, has the longest fluorescence lifetime (8.1 ns in toluene and 4.1 ns in DMF), followed by **1,6-Thio-PDI** (6.3 ns in toluene, 2.1 ns in DMF), and finally **1,6,7-Thio-PDI** (4.4 ns in toluene and 2.0 ns in DMF).

Lippert-Mataga Approximation

In order to gain further insight into the excited state properties of the different derivatives, the solvochromatic dependence of the absorption and emission spectra were analyzed by the Lippert-Mataga approximation to estimate the difference in dipole moment ($\Delta\mu$) between the ground (μ_g) and excited state (μ_e) via equation 1.[42] In the Lippert-Mataga approximation, the Stokes shift ($\bar{\nu}_a - \bar{\nu}_f$) of a fluorophore is proportional to the solvent orientation polarizability (Δf) which is determined from the solvent refractive index (n) and dielectric constant (ε). In equation 1, h and c have their usual meanings as Plank's constant and the speed of light, and a_o is the radius of the cavity in which the fluorophore resides.

$$\bar{\nu}_a - \bar{\nu}_f = \frac{2}{hca_o^3}\left(\frac{\epsilon-1}{2\epsilon+1} - \frac{n^2-1}{2n^2+1}\right)\left(\mu_e - \mu_g\right)^2 = \frac{2\Delta f}{hca_o^3}\Delta\mu^2 \quad (1)$$

The Stokes shift for each of the derivatives as a function of the solvent orientation polarizability (Δf) is shown in Figure S10 along with the linear regressions. The positive slope obtained for each of the isomers indicate that there is a larger excited state dipole moment than ground state dipole moment.[42] The resulting change in dipole moments for the three derivatives calculated from equation 1, and using a molecular radius estimated from DFT models (vide infra), are shown in Table 2. The slope of the solvent dependence for **1,6–Thio–PDI** is the largest relative to the other derivatives, predicting a 8.3 Debye the change in dipole moment. In comparison, the **1,7-** and **1,6,7-Thio-PDI** exhibit similar, but smaller dipole moment changes of 7.2 and 7.1

Debye respectively. To the best of our knowledge, this is the first example comparing the change in dipole moment change of a tri-substituted PDI (**1,6,7-Thio-PDI**).

Table 2. Dipole Moment Changes Derived by the Lippert–Mataga Analysis

PDI	$\Delta\mu = \mu_e - \mu_g$ **(Debye)**
1,6–Thio–PDI	8.3 ± 0.8
1,7–Thio–PDI	7.3 ± 0.7
1,6,7–Thio–PDI	7.1 ± 0.9

The change in dipole moments for these Thio–PDIs are comparable to others reported in the literature utilizing the Lippert-Mataga approximation where a comparison has been made between 1,6– and 1,7– regioisomers. A 1,6-difluorenyl-PDI, with swallowtail functionalities at the imide positions, exhibited a slightly larger dipole moment change of 9.64 D than the 1,7-regioisomer ($\Delta\mu$ = 8.65 D).[35] Similarly, a dialkylamino–substituted PDI, with cyclohexyl functionalities at the imide position, exhibited a larger change in dipole moment for the 1,6-(12.7 D) than the 1,7- PDI (7.9 D).[43] These trends were also observed for octyleamino–substituted PDIs.[44]

Density Functional Theory Modeling

Density functional theory (DFT) calculations were performed on the three derivatives to help understand any differences in excited state properties. The geometry of the derivatives were optimized at the CAM-B3LYP/cc-pVTZ level using a polarized continuum model (PCM) with THF as the solvent. Finally, time dependent DFT (TDDFT) calculations were performed at the CAM-B3LYP/may-cc-pVTZ level, with a PCM solvation model for THF, to predict the electronic absorption spectra and change in dipole moments. CAM-B3LYP was chosen as the functional due to its ability to reasonably predict the charge transfer properties of electronic transitions and estimates for the dipole moments.[45]

The optimized structures for the three derivatives, and their frontier molecular orbitals, are shown in Figure 4 and the twist angles of the perylene cores are included in Table 1. The perylene core of **1,6-Thio–PDI** is twisted along the N,N' axis due to the presence of the bay thio groups, which extend to either side of the perylene plane. The slight asymmetry of substitution on one half of the perylene core results in a ground state dipole moment of 4.2 Debye oriented along the N,N' axis, from the thio–functionalized side towards the unfunctionalized end. The perylene core of **1,7-Thio–PDI** is also twisted, however the thioether groups now point towards one face of the perylene. This results in a dipole moment of 2.8 Debye oriented towards the thioether side, normal to the plane of the perylene core. The perylene core of **1,6,7-Thio–PDI** shows the greatest degree of twist due to the proximity of the thioether groups at the 6 and 7 positions. This derivative has a 3.8 Debye dipole moment that nearly normal to the plane of the perylene, but tilted slight towards the 6,7– positions.

The frontier molecular orbital diagrams are shown in Figure 4 and are consistent with typical DFT calculations of PDIs, with π delocalization across the core and lack of orbital density at the imide nitrogens. Figure S11 shows a plot of the energetic levels of the frontier molecular orbitals for the three Thio–PDIs. Figure 5 shows the predicted electronic absorption spectra of the three derivatives from TDDFT calculations. The TDDFT results qualitatively reproduce the visible absorption spectra of each of the derivatives and help understand the differences between

them. All three spectra are dominated by a singlet π–π* transition ($S_0 \rightarrow S_1$), in the 500 nm range, which are associate primarily with the HOMO and LUMO orbitals shown in Figure 4 and Table S1. The HOMO of both **1,6-Thio–PDI** and **1,7-Thio–PDI** contain significant contribution from the sulfur atoms, which is absent in the LUMOs. This suggests there is a small amount of charge transfer from the sulfur atoms of the thioether groups towards the perylene core and is consistent with the change in dipole moments estimated from the Lippert–Mataga approximation. The HOMO of **1,6,7-Thio–PDI** only has significant contribution from the sulfur thio group in the 1 position. The twisting of the thio groups in the 6– and 7– positions, due to steric constrains, likely diminishes their sulfur orbital contribution to the HOMO.

The TDDFT results predict the $S_0 \rightarrow S_2$ transition for **1,6–Thio–PDI** and **1,6,7–Thio–PDI** in the 420nm range. These transitions overlap with the $S_0 \rightarrow S_1$ states and likely explain the broader absorption features seen in Figure 3. The $S_0 \rightarrow S_2$ transition for **1,7–thio–PDI** is predicted to be at 360 nm and is consistent with the second higher energy absorption feature around 400 nm as seen in, as well as the narrower absorption band at 560 nm.

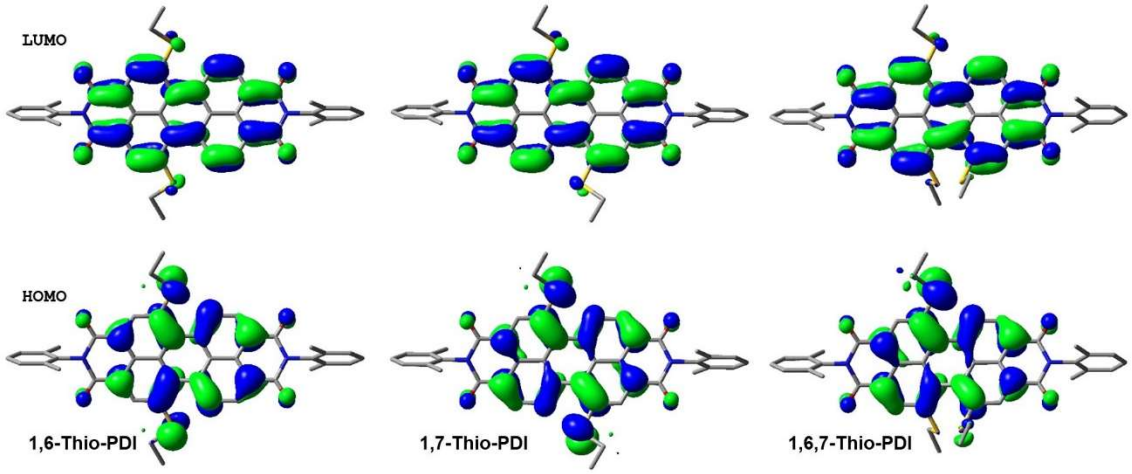

Figure 4. Optimized molecular structures and frontier molecular orbitals for the three derivatives, **1,6-Thio-PDI** (left), **1,7-Thio-PDI** (center), and **1,6,7-Thio-PDI** (right). The highest occupied (HOMO) and lowest unoccupied molecular orbitals (LUMO) are shown on the bottom and top respectively.

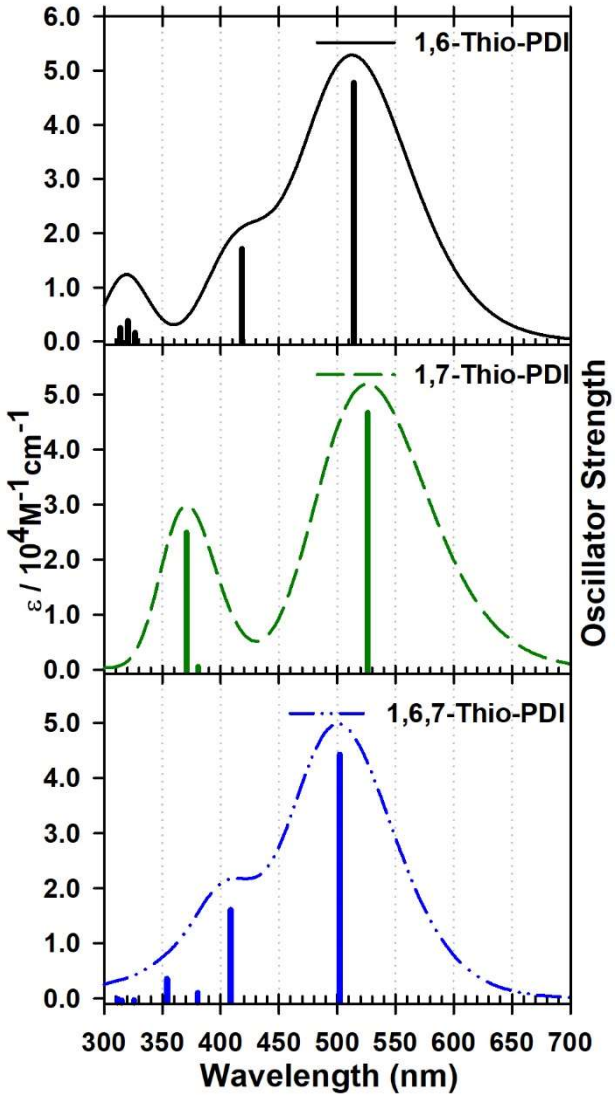

Figure 5. Predicted electronic absorption spectra of **1,6-Thio-PDI** (top), **1,7-Thio-PDI** (middle), and **1,6,7-Thio-PDI** (bottom) from TDDFT calculations at the CAM–B3LYP/may–cc–pVTZ/PCM(THF) level of theory. The simulated absorption spectra were generated using a 2000 cm^{-1} bandwidth for all peaks. The solid vertical lines correspond to the oscillator strengths of the calculated singlet transitions.

Electrochemistry

The electrochemical properties of the different derivatives were determined by cyclic voltammetry (CV) in tetrahydrofuran. All three Thio-PDIs undergo two electrochemically reversible reductions in the range -1 to -1.6 V vs ferrocene/ferrocinium as shown in Table 3 and Figure S12. There some subtle shifts in the potentials between derivatives, but the reductions follow trends reported for other PDI compounds.[2,21,46–48] All three Thio–PDIs show a separation of approximately 330 mV between the $E_{½}^{0/-1}$ and $E_{½}^{-1/-2}$ values.

Table 3. Electrochemical Parameters for Thio-PDI Derivatives [a]		
	$E_{½}^{0/-1}$	$E_{½}^{-1/-2}$
1,6-Thio-PDI	-1.21	-1.56
1,7-Thio-PDI	-1.28	-1.62
1,6,7-Thio-PDI	-1.15	-1.49
[a] V vs $Fc^{0/+}$		

Electronic Absorption of Reduced States

PDIs are known to produce anionic and dianonic redox states with vastly different electronic absorption spectra.[37,46,49] In order to determine the absorption spectra of the different Thio–PDI derivatives, in situ chemical reduction with Na(Hg), in the presence of 18–crown–6, was employed to produce the singly and doubly reduced states. These conditions allowed for the clean conversion between redox states of the Thio–PDIs. The absorption spectra of the Thio-PDIs in THF and the corresponding visual color changes are shown in Figure 6. The absorbance peaks of the neutral, singly reduced, and doubly reduced states follow a similar trend for all three Thio-PDIs and are consistent with previously reported 1,6– and 1,7–diadamantylthio–PDIs.[37]

The absorbance spectra for neutral complexes in THF are dominated by the broad peaks in the 500–600 nm range, resulting in an intense magenta to purple color. Reduction of the Thio–PDIs to the singly reduced state results in a significant red–shift of the main absorption bands to approximately 750 nm and increase in absorptivity. Additional lower intensity bands are also present from 800–1000 nm. Further reduction to the doubly reduced state results in a significant blue shift of the main absorption band back to the visible region, between 575–625 nm.

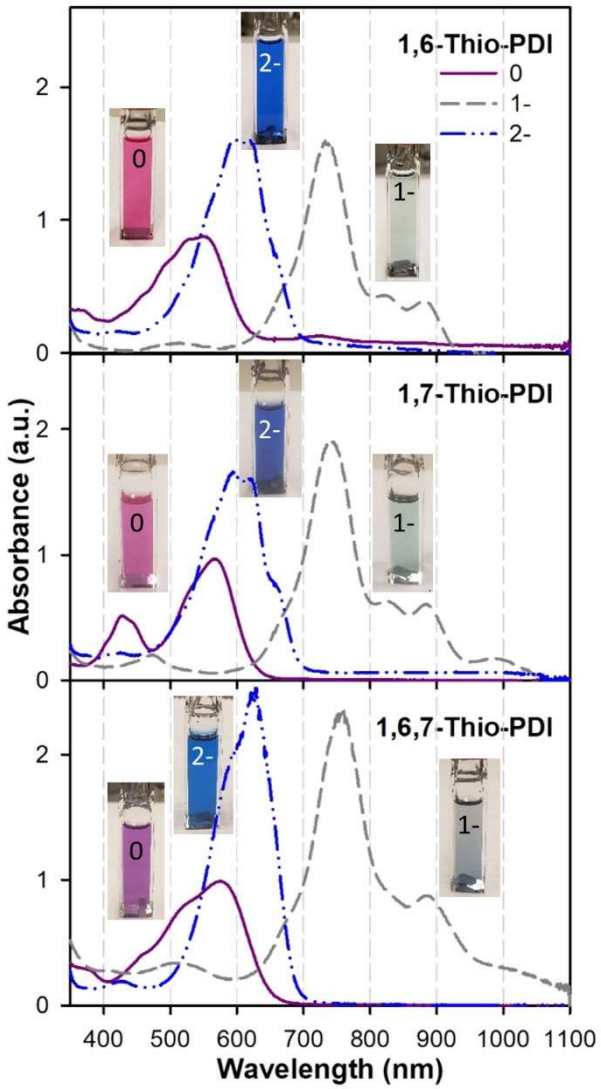

Figure 6. UV−Vis–NIR absorption spectra of **1,6-Thio-PDI** (top), **1,7-Thio-PDI** (middle) and **1,6,7-Thio-PDI** (bottom) recorded in THF with 0.01 M 18-crown-6. The singly and doubly reduced states were generated by chemical reduction using Na(Hg). The spectra of neutral states are shown as solid purple line, the singly reduced states as dashed grey lines, and the doubly reduced states as a dashed–dotted blue line. Included with the spectra are images of the cuvettes corresponding to the sample spectra.

Figure 6 also includes photographs of the samples, taken during the reduction process, highlighting the perceptible color changes of the Thio-PDIs between the neutral, singly reduced, and doubly reduced states. While there were some slight variations in perceivable color across the different Thio-PDIs redox states, similar trends were observed. The neutral state for all derivatives shows a pink to purple color, the singly reduced state is light green or blue, and the doubly reduced state is dark blue. These color changes for the 1,6-, 1,7-, and 1,6,7-Thio-PDIs correspond to what has been previous cited in literature in for 1,6- and 1,7- bay substituted adamantylthio derivatives in which distinct visual color changes were observed for 1,6- and 1,7-

with the doubly reduced state being a dark blue,[37] which is similar to the doubly reduced Thio-PDIs. Figure 7 shows the CIE (Commission Internationale de l'Eclairage) 1931 xy chromaticity diagram with the values calculated for each of the three Thio–PDI's in the neutral, singly and doubly reduced states. As expected, based on the similarities of images shown in Figure 6, the *xy* chromaticity values for the specific redox states are grouped together. The large difference in color between redox states highlights their potential use in electrochromic materials.

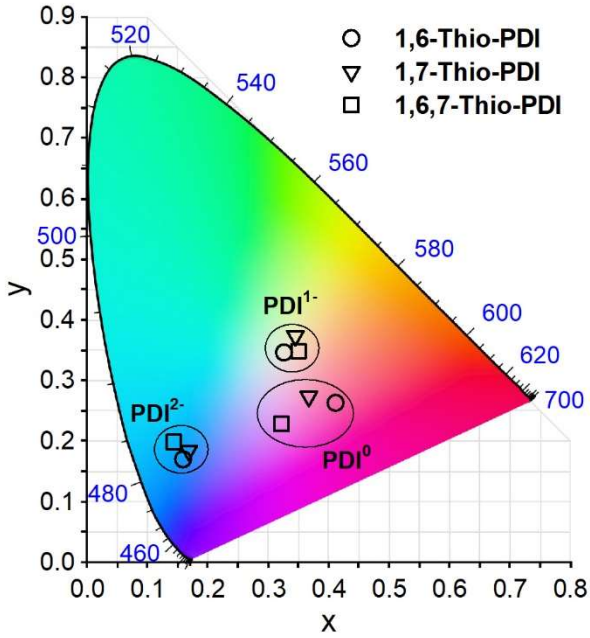

Figure 7. CIE 1931 xy chromaticity diagram with points calculated for the neutral, singly and doubly reduced forms of the Thio–PDIs.

Conclusion

In conclusion, we have described the synthesis, separation, and characterization of 1,6-, 1,7-, and 1,6,7- derivatives of dodecylthio–N,N'–(2,4–diisopropylphenyl)-3,4,9,10-perylenetetracarboxylic diimide. The three derivatives, **1,6-Thio-PDI**, **1,7-Thio-PDI,** and **1,6,7-Thio-PDI,** display noticeable differences in their photophysical properties, especially their fluorescence quantum yield and lifetimes. To the best of our knowledge, this is the first example of a tri–substituted thio–PDI that has been synthesized and fully characterized. The difference in dipole moment between the ground and excited states, estimated by the Lippert-Mataga analysis of solvent dependent absorption and emission properties, highlights the different excited state properties between the derivatives. We intend to further examine the difference in charge–transfer character of these derivatives using Stark (electroabsorption) spectroscopy. As others who have characterized isomers of bay–substituted PDIs, the noticeable differences in photophysical properties of the three different derivatives provides a cautionary warning to anyone working with these chromophores to ensure isomerically pure materials. Cyclic voltammetry showed minor differences in the reduction potentials for the singly and doubly reduced states. The absorption spectra of the singly and doubly reduced states are also reported, and show significantly different colors, highlighting their potential application in electrochromic materials.

Experimental section

General Methods and Materials. ^{1}H-NMR spectra were obtained on a Varian 500 MHz spectrometer and referenced to the solvent peak. LR and HR-ESI MS were obtained on a Thermo Electron Finnigan TSQ Quantum Ultra. Solvents, ACS grade or better, were purchased from Sigma Aldrich or Fischer Scientific and used as received unless specified otherwise. Brominated perylene-3,4,9,10-tetracarboxylic dianhydride (**Br-PTCDA**) was synthesized in a method similar to literature methods[29] and was available from previous projects.[18]

Imidization of Br-PTCDA. A suspension of **Br-PTCDA** (2.0 g, ~3.64 mmol) was mixed with 2,6-diisopropylanaline (2.2 mL, 11.28 mmol) in propionic acid (40 mL) and refluxed at 140˚C under nitrogen for 10 h. The reaction progress was monitored by thin layer chromatography ($CHCl_3$ with 1% CH_3OH), and following completion of the reaction, the solvent was evaporated. The crude product was purified by silica–gel column chromatography using chloroform. At this point, thin layer chromatography showed spots that corresponded to **1,6–Br–PDI**, **1,7-Br-PDI**, and **1,6,7-Br-PDI**, but the derivatives were not resolved at this step. ^{1}H NMR in $CDCl_3$ was consistent with previous reports,[30] and revealed **1,6-Br-PDI**, **1,7-Br-PDI**, and **1,6,7-Br-PDI** derivatives formed in a ratio of approximately 5:1:1. **1,6-Br-PDI** and **1,7-Br-PDI** LR-ESI m/z calculated for $C_{48}H_{41}Br_2N_2O_4$ $[MH]^+$ 867.14, found $[MH]^+$ 867.15; **1,6,7-Br-PDI** LR-ESI m/z calculated for $C_{48}H_{40}Br_3N_2O_4$ $[MH]^+$ 945.05, found $[MH]^+$ 947.06.

1,6-Thio–PDI, 1,7-Thio–PDI, and 1,6,7-Thio–PDI. A mixture of **Br–PDI** isomers (577.0 mg, 0.664 mmol), dodecylthiol (0.746 mL, 3.11 mmol), NaOH (100 mg) where was added to 30 mL of pyridine and reflexed under nitrogen for 4 hours. The reaction mixture was poured into 200 ml of 10 % (v) HCl and was extracted with DCM and the organic layers dried with $NaSO_4$. Isomeric products were separated via flash silica–gel column chromatography involving a 1:1 mixture of DCM and hexanes, and finally preparatory thin layer chromatography involving a 4:1 mixture of DCM and hexanes.

1,6-bis(dodecylthio)–N,N'–(2,4–diisopropylphenyl)-perylene diimide (1,6-Thiol-PDI): ^{1}H NMR (500mHz, $CDCl_3$): δ = 8.91 (d, *J* = 8.0 Hz, 2H), 8.86 (d, *J* = 8.0 Hz, 2H), 8.77 (s, 2H), 7.51 (m, 2H), 7.37 (d, *J* = 7.9 Hz, 4H), 3.25 (t, J =7.3, 2H), 2.78 (m, 4H), 2.68 (t, J = 7.5, 2H), 1.68 (m, 4H), 1.10-1.45 (m, 66 H). LR-ESI MS *m/z* calculated for $[MH]^+$ 1111.64, found $[MH]^+$ 1111.64. HR-ESI MS *m/z* calculated for $[MH]^+$ 1111.6434, found $[MH]^+$ 1111.6415 (1.7094 ppm).

1,7-bis(dodecylthio)–N,N'–(2,4–diisopropylphenyl)-perylenediimide (1,7-Thiol-PDI): ^{1}H NMR (500 mHz, $CDCl_3$): 8.94 (d, *J* = 8.0 Hz, 2H), 8.86 (s, 2H) 8.75 (d, *J* = 8.0 Hz, 2H), 7.51 (t, *J* = 7.6 Hz, 2H), 7.37 (d, *J* = 7.8 Hz, 4H), 3.26 (t, J = 7.4, 4H), 2.79 (m, 4H), 1.70 (m, 4H), 1.10-1.07 (m, 66 H). LR-ESI MS *m/z* calculated for $[MH]^+$ 1111.64, found $[MH]^+$ 1111.64. HR-ESI MS *m/z* calculated for $[MH]^+$ 1111.6434, found $[MH]^+$ 1111.6431 (1.5505 ppm).

1,6,7-tris(dodecylthio)–N,N'–(2,4–diisopropylphenyl)-perylenediimide (1,6,7-Thiol-PDI): ^{1}H NMR (500 mHz, $CDCl_3$): 8.93 (d, *J* = 8.3 Hz, 1H), 8.85 (s, 1H). 8.77 (m, 3H), 7.51 (t, 2H, *J* = 8.0), 7.37 (d, *J* = 7.7 Hz, 4H), 3.36 (m, 1H), 3.07 (m, 5H), 2.795 (septet, 4H), 1.78-0.96 (m, 84 H), 0.86 (t, *J* = 7.0, 9H). LR-ESI MS *m/z* calculated for $[MH]^+$ 1311.80, found $[MH]^+$ 1311.80. HR-ESI MS *m/z* calculated for $[MH]^+$ 1311.8035, found $[MH]^+$ 1311.8013 (1.6439 ppm).

Electronic Absorption and Emission Spectroscopy. UV–Vis electronic absorption spectra were taken on a Perkin-Elmer Lambda 950 UV–vis spectrometer or an Agilent 8453A

spectrometer running Olisworks software. Samples were background subtracted using a quartz cuvette. Steady–state fluorescence spectra were taken on Horiba Fluorolog-3 Model FL3-21. Solution fluorescence spectra were obtained at a right-angle detection. Fluorescence lifetimes were measured by phase modulated frequency-domain lifetime using a Horiba FluoroLog-Tau3 spectrometer. To remove stray light and fluorescence from other sources, a 600 nm long pass filter was used on the detector side. All solutions were purged with nitrogen gas to remove oxygen prior to steady-state and lifetime fluorescence measurements. A selection of phase-modulated data and fits are included in the Supporting Information.

Computational Details. Geometry optimizations for the Thio–PDI derivatives were carried out using density functional theory (DFT) as implemented in Gaussian09, revision D.01[50] at the Computational Center for Nanotechnology Innovations at Rensselaer Polytechnic Institute. The CAM–B3LYP functional[45] was used with the cc–pVTZ basis set for geometry optimizations in the gas phase, followed by optimizations that included the effect of solvation by THF using the self–consistent reaction field (SCRF) of polarizable continuum model (PCM)[51] approach. The resulting structures were confirmed as minima using frequency calculations at the same level of theory. Single point energy and TDDFT calculations were performed on the solvent-phase optimized structure at the CAM–B3LYP/may–cc–pVTZ/PCM(THF) level of theory.

Cyclic Voltammetry. Cyclic volmmetric studies were carried out using an CHI440a potentiostat under an atmosphere of N_2 using a three-electrode arrangement in a single compartment cell. A glassy carbon working electrode, an Ag wire pseudo reference electrode, and a Pt counter electrode. The electrolyte consisted of 0.1 M tetra(n–butyl)ammonium hexaphlorophasphate in anhydrous tetrahydrofuran. Redox potentials are quoted versus the ferrocenium-ferrocene couple used as an internal reference.[52]

Chemical Reductions. Chemical reductions studies were carried out manner similar to a previous method,[53] using a quartz cuvette with the 1 cm optical path length. Samples were prepared in a N_2 purged glovebox in anhydrous THF. Chemical reduction was achieved by using small additions of Na(10%)–Hg with a slight excess of 18-crown-6 added to aid in the solubility of Na+ ions under air-free conditions. Clean conversion between the different redox states was confirmed by the appearance of isosbestic points.

Acknowledgment. This work was supported in part by Rensselaer Polytechnic Institute and by the National Science Foundation under Contract CHE–1255100 and CHE–1905064. We acknowledge Kiran Ahmed for assisting in the CIE colorimetry calculations and the ACS Project SEED for supporting her work.

Supporting Information

Mass spectra, ^{1}H NMR, fluorescence quantum yield data, frequency-domain fluorescence lifetime measurements, Lippert–Mataga analysis of Stoke's shifts, cyclic voltammograms, results of TD–DFT excited state calculations, nuclear coordinates of minimum-energy geometries for **1,6-Thio-PDI**, **1,7–Thio–PDI** and **1,6,7–Thio–PDI**.

TOC Graphic

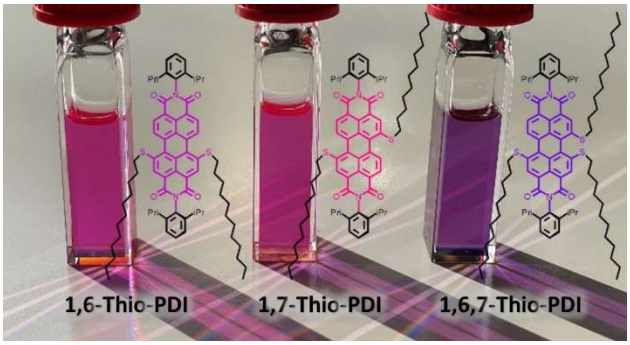

References

(1) Huang, C.; Barlow, S.; Marder, S. R. Perylene-3,4,9,10-Tetracarboxylic Acid Diimides: Synthesis, Physical Properties, and Use in Organic Electronics. *J. Org. Chem.* **2011**, *76*, 2386–2407.

(2) Würthner, F. Perylene Bisimide Dyes as Versatile Building Blocks for Functional Supramolecular Architectures. *Chem. Commun.* **2004**, *4*, 1564–1579.

(3) Herbst, W.; Ed, K. H. *Industrial Organic Pigments: Production, Properties, Applications*, 2nd ed.; WILEY-VCH: Weinheim, 1997.

(4) Margineanu, A.; Hofkens, J.; Cotlet, M.; Habuchi, S.; Stefan, A.; Qu, J.; Kohl, C.; Mu, K.; Vercammen, J.; Engelborghs, Y.; Gensch, T.; Schryver, F. C. De. Photophysics of a Water - Soluble Rylene Dye : Comparison with Other Fluorescent Molecules for Biological Applications. *J. Phys. Chem. B* **2004**, *108*, 12242–12251.

(5) Jung, M.; Smoother, T.; Martin, A. A.; Mcdonagh, A. M.; Maynard, P. J.; Lennard, C.; Roux, C. Fluorescent TiO 2 Powders Prepared Using a New Perylene Diimide Dye : Applications in Latent Fingermark Detection. *Forensic Sci. Int.* **2007**, *173*, 154–160.

(6) Rappold, M.; Warttinger, U.; Krämer, R. A Fluorescent Probe for Glycosaminoglycans Applied to the Detection of Dermatan Sulfate by a Mix-and-Read Assay. *Mol. 2017, Vol. 22, Page 768* **2017**, *22*, 768.

(7) Yukruk, F.; Dogan, A. L.; Canpinar, H.; Guc, D.; Akkaya, E. U. Water-Soluble Green Perylenediimide (PDI) Dyes as Potential Sensitizers for Photodynamic Therapy. *Org. Lett.* **2005**, *7*, 2885–2887.

(8) Zhang, E.; Liu, L.; Lv, F.; Wang, S. Design and Synthesis of Reactive Perylene Tetracarboxylic Diimide Derivatives for Rapid Cell Imaging. *ACS Omega* **2018**, *3*, 8691–8696.

(9) Würthner, F.; Nowak-Król, A. Progress in the Synthesis of Perylene Bisimide Dyes. *R. Soc. Chem.* **2019**, *6*, 1272–1318.

(10) Lee, S. K.; Zu, Y.; Herrmann, A.; Geerts, Y.; Bard, A. J.; December, R. V; Müllen, K.; Bard, A. J. Electrochemistry, Spectroscopy and Electrogenerated Chemiluminescence of Perylene, Terrylene, and Quaterrylene Diimides in Aprotic Solution. *J. Am. Chem. Soc.* **1999**, *121*, 3513–3520.

(11) Tintori, F.; Laventure, A.; Welch, G. C. Perylene Diimide Based Organic Photovoltaics with Slot-Die Coated Active Layers from Halogen-Free Solvents in Air at Room Temperature. *ACS Appl. Mater. Interfaces* **2019**, *11*, 39010–39017.

(12) Qin, R.; Guo, D.; Li, M.; Li, G.; Bo, Z.; Wu, J. Perylene Monoimide Dimers Enhance Ternary Organic Solar Cells Efficiency by Induced D-A Crystallinity. *ACS Appl. Energy Mater.* **2019**, *2*, 305–311.

(13) Kozma, E.; Catellani, M. Perylene Diimides Based Materials for Organic Solar Cells. *Dye. Pigment.* **2013**, *98*, 160–179.

(14) Keum, C.; Becker, D.; Archer, E.; Bock, H.; Kitzerow, H.; Gather, M. C.; Murawski, C. Organic Light-Emitting Diodes Based on a Columnar Liquid-Crystalline Perylene Emitter. *Adv. Opt. Mater.* **2020**, *8*, 2000414.

(15) Li, G.; Zhao, Y.; Li, J.; Cao, J.; Zhu, J.; Sun, X. W.; Zhang, Q. Synthesis, Characterization, Physical Properties, and OLED Application of Single BN-Fused Perylene Diimide. *J. Org. Chem.* **2015**, *80*, 196–203.

(16) Ahrens, M. J.; Sinks, L. E.; Rybtchinski, B.; Liu, W.; Jones, B. A.; Giaimo, J. M.; Gusev, A. V.; Goshe, A. J.; Tiede, D. M.; Wasielewski, M. R. Self-Assembly of Supramolecular

Light-Harvesting Arrays from Covalent Multi-Chromophore Perylene-3,4:9,10-Bis(Dicarboximide) Building Blocks. *J. Am. Chem. Soc.* **2004**, *126*, 8284–8294.
(17) Inan, D.; Dubey, R. K.; Jager, W. F.; Grozema, F. C. Tailoring Photophysical Processes of Perylene-Based Light Harvesting Antenna Systems with Molecular Structure and Solvent Polarity. *J. Phys. Chem. C* **2019**, *123*, 36–47.
(18) Beauvilliers, E. E.; Topka, M. R.; Dinolfo, P. H. Synthesis and Characterization of Perylene Diimide Based Molecular Multilayers Using CuAAC: Towards Panchromatic Assemblies. *RSC Adv.* **2014**, *4*, 32866.
(19) Zhang, B.; Soleimaninejad, H.; Jones, D. J.; White, J. M.; Ghiggino, K. P.; Smith, T. A.; Wong, W. W. H. Highly Fluorescent Molecularly Insulated Perylene Diimides: Effect of Concentration on Photophysical Properties. *Chem. Mater.* **2017**, *29*, 8395–8403.
(20) Zhang, B.; Zhao, P.; Wilson, L. J.; Subbiah, J.; Yang, H.; Mulvaney, P.; Jones, D. J.; Ghiggino, K. P.; Wong, W. W. H. High-Performance Large-Area Luminescence Solar Concentrator Incorporating a Donor-Emitter Fluorophore System. *ACS Energy Lett.* **2019**, *4*, 1839–1844.
(21) Ahrens, M. J.; Fuller, M. J.; Wasielewski, M. R. Cyanated Perylene-3,4-Dicarboximides and Perylene-3,4:9,10-Bis(Dicarboximide): Facile Chromophoric Oxidants for Organic Photonics and Electronics. *Chem. Mater.* **2003**, *15*, 2684–2686.
(22) Zhan, X.; Tan, Z.; Domercq, B.; An, Z.; Zhang, X.; Barlow, S.; Li, Y.; Zhu, D.; Kippelen, B.; Marder, S. R. A High-Mobility Electron-Transport Polymer with Broad Absorption and Its Use in Field-Effect Transistors and All-Polymer Solar Cells. *J. Am. Chem. Soc.* **2007**, *129*, 7246–7247.
(23) Zafer, C.; Kus, M.; Turkmen, G.; Dincalp, H.; Demic, S.; Kuban, B.; Teoman, Y.; Icli, S. New Perylene Derivative Dyes for Dye-Sensitized Solar Cells. *Sol. Energy Mater. Sol. Cells* **2007**, *91*, 427–431.
(24) Erten-Ela, S.; Turkmen, G. Perylene Imide Dyes for Solid-State Dye-Sensitized Solar Cells: Spectroscopy, Energy Levels and Photovoltaic Performance. *Renew. Energy* **2011**, *36*, 1821–1825.
(25) Shibano, Y.; Umeyama, T.; Matano, Y.; Imahori, H. Electron-Donating Perylene Tetracarboxylic Acids for Dye-Sensitized Solar Cells. *Org. Lett.* **2007**, *9*, 1971–1974.
(26) Yao, J.; Qiu, B.; Zhang, Z.; Xue, L.; Wang, R.; Zhang, C.; Chen, S.; Zhou, Q.; Sun, C.; Yang, C.; Xiao, M.; Meng, L.; Li, Y. Cathode Engineering with Perylene-Diimide Interlayer Enabling over 17% Efficiency Single-Junction Organic Solar Cells. *Nat. Commun.* **2020**, *11*, 1–10.
(27) Schnurpfeil, G.; Stark, J.; Whrle, D. Syntheses of Uncharged , Positively and Negatively Charged 3,4,9,10-Perylene-Bis(Dicarboximides). *Dye. Pigment.* **1995**, *27*, 339–350.
(28) Langhals, H. Control of the Interactions in Multichromophores: Novel Concepts. Perylene Bis-Imides as Components for Larger Functional Units. *Helv. Chim. Acta* **2005**, *88*, 1309–1343.
(29) Böhm, A.; Arms, H.; Henning, G.; Blaschka, P. 1,7-Diaroxy-or -Arylthio-Substituted Perylene-3,4,9,10-Tetracarboxylic Acids, Their Dianhydrides and Diimides. DE19547209A1, 1997.
(30) Würthner, F.; Stepanenko, V.; Chen, Z.; Saha-Möller, C. R.; Kocher, N.; Stalke, D. Preparation and Characterization of Regioisomerically Pure 1,7-Disubstituted Perylene Bisimide Dyes. *J. Org. Chem.* **2004**, *69*, 7933–7939.
(31) Dubey, R. K.; Efimov, A.; Lemmetyinen, H. 1,7-And 1,6-Regioisomers of Diphenoxy and

Dipyrrolidinyl Substituted Perylene Diimides: Synthesis, Separation, Characterization, and Comparison of Electrochemical and Optical Properties. *Chem. Mater.* **2011**, *23*, 778–788.
(32) Dubey, R. K.; Niemi, M.; Kaunisto, K.; Stranius, K.; Efimov, A.; Tkachenko, N. V.; Lemmetyinen, H. Excited-State Interaction of Red and Green Perylene Diimides with Luminescent Ru(II) Polypyridine Complex. *Inorg. Chem.* **2013**, *52*, 9761–9773.
(33) Fan, L.; Xu, Y.; Tian, H. 1,6-Disubstituted Perylene Bisimides: Concise Synthesis and Characterization as near-Infrared Fluorescent Dyes. *Tetrahedron Lett.* **2005**, *46*, 4443–4447.
(34) Dey, S.; Efimov, A.; Lemmetyinen, H. Diaryl-Substituted Perylene Bis(Imides): Synthesis, Separation, Characterization and Comparison of Electrochemical and Optical Properties of 1,7-and 1,6-Regioisomer. *European J. Org. Chem.* **2012**, *2012*, 2367–2374.
(35) Kozma, E.; Mróz, W.; Andicsová Eckstein, A.; Lukeš, V.; Galeotti, F.; Šišková, A.; Danko, M.; Catellani, M. A Joint Experimental and Theoretical Study on the Electro-Optical Properties of 1,6- and 1,7-Fluorenyl Disubstituted Perylene Diimide Isomers. *New J. Chem.* **2018**, *42*, 1061–1066.
(36) Handa, N. V; Mendoza, K. D.; Shirtcliff, L. D. Syntheses and Properties of 1,6 and 1,7 Perylene Diimides and Tetracarboxylic Dianhydrides. *Org. Lett.* **2011**, *13*, 4724–4727.
(37) Slater, A. G.; Stephen Davies, E.; Argent, S. P.; Lewis, W.; Blake, A. J.; Mcmaster, J.; Champness, N. R. Bis-Thioether-Substituted Perylene Diimides: Structural, Electrochemical, and Spectroelectrochemical Properties. *J. Org. Chem.* **2013**, *78*, 2853−2862.
(38) Ma, J.; Yin, L.; Zou, G.; Zhang, Q. Regioisomerically Pure 1 , 7-Dibromo-Substituted Perylene Bisimide Dyes : Efficient Synthesis , Separation , and Characterization. *European J. Org. Chem.* **2015**, *2015*, 3296–3302.
(39) Dubey, R. K.; Niemi, M.; Kaunisto, K.; Efimov, A.; Tkachenko, N. V.; Lemmetyinen, H. Direct Evidence of Significantly Different Chemical Behavior and Excited-State Dynamics of 1,7- and 1,6-Regioisomers of Pyrrolidinyl-Substituted Perylene Diimide. *Chem. - A Eur. J.* **2013**, *19*, 6791–6806.
(40) Liu, Y.; Li, Y.; Jiang, L.; Gan, H.; Liu, H.; Li, Y.; Zhuang, J.; Lu, F.; Zhu, D. Assembly and Characterization of Novel Hydrogen-Bond-Induced Nanoscale Rods. *J. Org. Chem.* **2004**, *69*, 9049–9054.
(41) Feng, J.; Wang, D.; Wang, H.; Zhang, D.; Zhang, L.; Li, X. Structural and Property Comparison between the Di-Piperidinyl- and Di-Pyrrolidinyl-Substituted Perylene Tetracarboxylic Diimides. *J. Phys. Org. Chem.* **2011**, *24*, 621–629.
(42) Lakowicz, J. R. (University of M. S. of M. *Principles of Fluorescence Spectroscopy*, 3rd ed.; Springer, 2006.
(43) Chen, K. Y.; Chang, C. W.; Tsai, H. Y. 1,6-and 1,7-Regioisomers of Highly Soluble Amino-Substituted Perylene Tetracarboxylic Dianhydrides: Synthesis, Optical and Electrochemical Properties. *Materials (Basel).* **2015**, *8*, 4943–4960.
(44) Ahrens, M. J.; Tauber, M. J.; Wasielewski, M. R. Bis(n-Octylamino)Perylene-3,4:9,10-Bis(Dicarboximide)s and Their Radical Cations:Â€‰ Synthesis, Electrochemistry, and ENDOR Spectroscopy. *J. Org. Chem.* **2006**, *71*, 2107–2114.
(45) Yanai, T.; Tew, D. P.; Handy, N. C. A New Hybrid Exchange-Correlation Functional Using the Coulomb-Attenuating Method (CAM-B3LYP). *Chem. Phys. Lett.* **2004**, *393*, 51–57.

(46) Gosztola, D.; Niemczyk, M. P.; Svec, W.; Lukas, A. S.; Wasielewski, M. R. Excited Doublet States of Electrochemically Generated Aromatic Imide and Diimide Radical Anions. *J. Phys. Chem. A* **2000**, *104*, 6545–6551.
(47) Zhao, Y.; Wasielewski, M. R. 3,4:9,10-Perylenebis(Dicarboximide) Chromophores That Function as Both Electron Donors and Acceptors. *Tetrahedron Lett.* **1999**, *40*, 7047–7050.
(48) Lukas, A. S.; Zhao, Y.; Miller, S. E.; Wasielewski, M. R. Biomimetic Electron Transfer Using Low Energy Excited States: A Green Perylene-Based Analogue of Chlorophyll A. *J. Phys. Chem. B* **2002**, *106*, 1299–1306.
(49) Ford, W. E.; Hiratsuka, H.; Kamat, P. V. Photochemistry of 3,4,9,10-Perylenetetracarboxylic Dianhydride Dyes. 4. Spectroscopic and Redox Properties of Oxidized and Reduced Forms of the Bis(2,5-Di-Tert-Butylphenyl)Imide Derivative. *J. Phys. Chem.* **2002**, *93*, 6692–6696.
(50) Frisch, M. J.; Trucks, G. W.; Schlegel, H. B.; Scuseria, G. E.; Robb, M. A.; Cheeseman, J. R.; Scalmani, G.; Barone, V.; Petersson, G. A.; Nakatsuji, H.; Li, X.; Caricato, M.; Marenich, A.; Bloino, J.; B. G. Janesko; Gomperts, R.; Mennucci, B.; Hratchian, H. P.; Ortiz, J. V.; Izmaylov, A. F.; Sonnenberg, J. L.; Williams-Young, D.; Ding, F.; Lipparini, F.; Egidi, F.; Goings, J.; Peng, B.; Petrone, A.; Henderson, T.; Ranasinghe, D.; Zakrzewski, V. G.; Gao, J.; Rega, N.; Zheng, G.; Liang, W.; Hada, M.; Ehara, M.; Toyota, K.; Fukuda, R.; Hasegawa, J.; Ishida, M.; Nakajima, T.; Honda, Y.; Kitao, O.; Nakai, H.; Vreven, T.; Throssell, K.; J. A. Montgomery, J.; Peralta, J. E.; Ogliaro, F.; Bearpark, M.; Heyd, J. J.; Brothers, E.; Kudin, K. N.; Staroverov, V. N.; Keith, T.; Kobayashi, R.; Normand, J.; Raghavachari, K.; Rendell, A.; Burant, J. C.; Iyengar, S. S.; Tomasi, J.; Cossi, M.; Millam, J. M.; Klene, M.; Adamo, C.; Cammi, R.; Ochterski, J. W.; Martin, R. L.; Morokuma, K.; Farkas, O.; Foresman, J. B.; Fox, D. J. Gaussian 09, Revision D.01, 2009.
(51) Tomasi, J.; Mennucci, B.; Cammi, R. Quantum Mechanical Continuum Solvation Models. *Chem. Rev.* **2005**, *105*, 2999–3093.
(52) Gagne, R. R.; Koval, C. A.; Lisensky, G. C. Ferrocene as an Internal Standard for Electrochemical Measurements. *Inorg. Chem.* **1980**, *19*, 2854–2855.
(53) Dinolfo, P. H.; Hupp, J. T. Tetra-Rhenium Molecular Rectangles as Organizational Motifs for the Investigation of Ligand-Centered Mixed Valency: Three Examples of Full Delocalization. *J. Am. Chem. Soc.* **2004**, *126*, 16814–16819.